

Computing Eigenmodes of Elliptic Operators Using Radial Basis Functions

Rodrigo B. Platte and Tobin A. Driscoll*

University of Delaware
Department of Mathematical Sciences
Ewing Hall, Newark, DE 19716, U.S.A.
{platte, driscoll}@math.udel.edu

August 1, 2003

Abstract

Radial basis function (RBF) approximations have been successfully used to solve boundary-value problems numerically. We show that RBFs can also be used to compute eigenmodes of elliptic operators. Particular attention is given to the Laplacian operator in two dimensions, including techniques to avoid degradation of the solution near the boundaries. For regions with corner singularities, special functions must be added to the basis to maintain good convergence. Numerical results compare favorably to basic finite element methods.

Keywords. radial basis functions, eigenvalues, numerical methods, Laplacian, corner singularities

*Supported by NSF grant DMS-0104229.

1 Introduction

Many positive properties of radial basis function (RBF) methods have been identified in connection with boundary-value problems (BVPs) [1, 2, 3, 4]. They are grid-free numerical schemes very suitable for problems in irregular geometries. They can exploit accurate and smooth representations of the boundary, are very easy to implement, and can be spectrally accurate [5, 6]. It would be expected that the benefits experienced by the use of RBFs in BVPs would carry over for eigenvalue problems. In this article we formulate and apply an RBF-based method to compute eigenmodes of elliptic operators.

Given a linear elliptic second order partial differential operator L and a bounded region Ω in \mathbb{R}^n with boundary $\partial\Omega$, we seek eigenpairs $(\lambda, u) \in (\mathbb{C}, C(\bar{\Omega}))$ satisfying

$$\begin{aligned} Lu + \lambda u &= 0 && \text{in } \Omega && \text{and} \\ L_B u &= 0 && \text{on } \partial\Omega, \end{aligned} \tag{1}$$

where L_B is a linear boundary operator of the form

$$L_B u = au + b(\mathbf{n} \cdot \nabla u). \tag{2}$$

Here a and b are given constants and \mathbf{n} is the unit outward normal vector defined on the boundary. We assume that Ω is open and that the eigenvalue problem is well-posed.

We use an interpolating RBF approximation of an eigenfunction of (1) and replace the eigenvalue problem above with a finite-dimensional eigenvalue problem. In order to compute the eigenpairs of the modified system, we approximate the operator L by a matrix that incorporates the boundary conditions and then

use standard techniques to find the eigenvalues and eigenvectors of this matrix.

As pointed out in [2, 7], straightforward RBF approximations are relatively inaccurate near the boundaries, and special attention should be given to this issue. We study the boundary clustering of nodes and the collocation of the PDE on the boundary and verify that they are effective techniques for preventing degradation of the solution near the edges of the domain.

We consider the effect of corner singularities in 2-D regions. It is known that some eigenfunctions are not smooth at corners with interior angle π/φ where φ is not integer. As a result a straightforward RBF approximation is severely degraded in this case. Several authors have exploited explicit information about the singular behavior of an eigenfunction at a corner to propose efficient algorithms to compute eigenvalue for these regions (see, for example, [8, 9, 10]). With these efforts as motivation, we append terms to the RBF expansion that approximate the singular behavior of an eigenfunction. To our knowledge this type of singular augmentation has not been used before with RBFs.

The remainder of this article is organized as follows: In the next section we introduce RBF approximations. In section 3 we formulate the problem in matrix form. In section 4 we present the boundary treatment techniques. In section 5 a scheme for regions with corner singularities is introduced. We carry out several experiments in 2-D regions for the Laplacian operator for a disk, an L-shaped region, and a rhombus as pictured in Fig. 1, and compare to finite elements and pseudospectral methods.

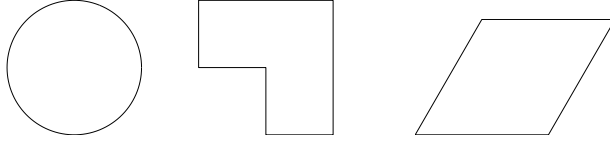


Figure 1: 2-D regions considered for the numerical experiments.

2 Radial basis functions

Let $\{\mathbf{y}_i\}_{i=1}^N$ be a finite set of distinct points in \mathbb{R}^n . Given a function ϕ from \mathbb{R}^+ to \mathbb{R} , we write the standard RBF approximation of a function u :

$$\tilde{u}(\mathbf{x}) \equiv \sum_{i=1}^N \alpha_i \phi(\|\mathbf{x} - \mathbf{y}_i\|_2), \quad \mathbf{x} \in \mathbb{R}^n. \quad (3)$$

The points \mathbf{y}_i are called centers and ϕ the radial basis function [11]. The coefficients α_i are chosen so that \tilde{u} satisfies certain interpolation criteria to be discussed later.

Several choices for ϕ have been presented in the literature [7, 11, 12]. Some of the most commonly used RBFs are:

$$\phi(r) = r^3, \quad (\text{cubic}),$$

$$\phi(r) = r^2 \log(r), \quad (\text{thin plate spline}),$$

$$\phi(r) = (1 - r)_+^m p(r), \quad (\text{Wendland functions [13], where } p \text{ is polynomial}),$$

$$\phi(r) = \exp(-cr^2), \quad (\text{Gaussian}),$$

$$\phi(r) = \sqrt{c^2 + r^2}, \quad (\text{multiquadric}),$$

where r is real and non-negative and c is a positive constant. The multiquadric, in particular, has been successfully used to solve elliptic problems numerically [2, 4]. It was introduced by Hardy [14], and Kansa applied it to solve PDEs in

the early 1990s [1].

In order to determine the coefficients α_i , a set of N distinct interpolation points in $\bar{\Omega}$ is needed. Usually, the same set of points is used for centers and interpolation. Taking centers outside the domain appropriately, however, has been shown to be an effective way of improving accuracy near the boundary — see, e.g., Fedoseyev et al. [2] and Fornberg et al. [7]. If $u(\mathbf{x}_j)$, $j = 1, 2, \dots, N$, were known, finding the α_i would require solution of an $N \times N$ linear system $A\boldsymbol{\alpha} = \mathbf{u}$, $A \equiv [\phi(\|\mathbf{x}_i - \mathbf{y}_j\|_2)]_{N \times N}$, $\boldsymbol{\alpha} \equiv [\alpha_1, \alpha_2, \dots, \alpha_N]^T$ and $\mathbf{u} \equiv [u(\mathbf{x}_1), u(\mathbf{x}_2), \dots, u(\mathbf{x}_N)]^T$. A is called the RBF interpolation matrix and, for some RBFs, is positive definite [11].

3 Algorithm

There are different ways to use (3) to derive a finite-dimensional eigenvalue problem. We shall start with the method we find the most efficient. The idea behind this scheme is to approximate the operator L by a matrix L_ϕ that also incorporates the boundary conditions.

For N_I nodes in the interior of the domain and N_B nodes on the boundary, $N = N_I + N_B$, we denote the interpolation points by $\{\mathbf{x}_i\}_{i=1}^{N_I} \in \Omega$ and $\{\mathbf{x}_i\}_{i=N_I+1}^N \in \partial\Omega$. In order to obtain L_ϕ , we enforce the boundary condition at every point \mathbf{x}_i on the boundary, and evaluate the RBF approximation (3) at the interior interpolation points to obtain

$$\begin{aligned} \sum_{i=0}^N \alpha_i \phi(\|\mathbf{x}_j - \mathbf{y}_i\|_2) &= \tilde{u}(\mathbf{x}_j), & j = 1, 2, \dots, N_I, \\ \sum_{i=0}^N \alpha_i L_B \phi(\|\mathbf{x}_j - \mathbf{y}_i\|_2) &= 0, & j = N_I + 1, N_I + 2, \dots, N. \end{aligned}$$

In the notation $L_B\phi(\|\mathbf{x}_j - \mathbf{y}_i\|_2)$ it is understood that L_B is applied to the first variable, then evaluated. This can be written in matrix form as

$$\boldsymbol{\alpha} = \mathcal{A}^{-1} \begin{bmatrix} \tilde{\mathbf{u}}^I \\ 0_{N_B \times 1} \end{bmatrix}, \quad (4)$$

where $\tilde{\mathbf{u}}^I \equiv [\tilde{u}(\mathbf{x}_1), \tilde{u}(\mathbf{x}_2), \dots, \tilde{u}(\mathbf{x}_{N_I})]^T$, $0_{p \times q}$ is the $p \times q$ zero matrix,

$$\mathcal{A} \equiv \begin{bmatrix} A^I \\ B \end{bmatrix}, \quad A^I \equiv \left[\phi(\|\mathbf{x}_i - \mathbf{y}_j\|_2) \right]_{N_I \times N}, \quad \text{and } B \equiv \left[L_B\phi(\|\mathbf{x}_{N_I+i} - \mathbf{y}_j\|_2) \right]_{N_B \times N}.$$

For the Dirichlet boundary condition, the matrix \mathcal{A} becomes the usual RBF interpolation matrix.

For the interior points, we also have that

$$\sum_{i=1}^N \alpha_i L\phi(\|\mathbf{x}_j - \mathbf{y}_i\|_2) = \lambda \tilde{u}(\mathbf{x}_j) \quad j = 1, 2, \dots, N_I,$$

which can be expressed as

$$L^I \boldsymbol{\alpha} = \lambda \tilde{\mathbf{u}}^I, \quad (5)$$

where

$$L^I \equiv \left[L\phi(\|\mathbf{x}_i - \mathbf{y}_j\|_2) \right]_{N_I \times N}.$$

Combining (4) and (5) we obtain

$$L_\phi \tilde{\mathbf{u}}^I = \lambda \tilde{\mathbf{u}}^I. \quad (6)$$

L_ϕ is the $N_I \times N_I$ matrix given by

$$L_\phi \equiv L^I \mathcal{A}^{-1} \begin{bmatrix} I_{N_I \times N_I} \\ 0_{N_B \times N_I} \end{bmatrix}.$$

Here $I_{p \times p}$ is the identity matrix of order p .

The RBF approximation of the eigenpairs of (1) is now obtained by computing the eigenvalues and eigenvectors of the matrix L_ϕ .

In some instances it is necessary or useful to add functions to the RBF approximation (3),

$$\tilde{u}(\mathbf{x}) \equiv \sum_{i=1}^N \alpha_i \phi(\|\mathbf{x} - \mathbf{y}_i\|_2) + \sum_{i=1}^M \beta_i g_i(\mathbf{x}), \quad \mathbf{x} \in \mathbb{R}^n. \quad (7)$$

To make this system uniquely solvable, it is usually required that

$$\sum_{i=1}^N \alpha_i g_j(\mathbf{x}) = 0, \quad j = 1, 2, \dots, M.$$

For the Neumann problem, augmentation by a constant is especially appropriate due to the trivial zero mode.

Repeating the procedure above for (7), one obtains the following expression for the operator of the finite-dimensional system:

$$L_\phi \equiv L_2^I \mathcal{A}_2^{-1} \begin{bmatrix} I_{N_I \times N_I} \\ 0_{(N_B+M) \times N_I} \end{bmatrix},$$

where

$$L_2^I \equiv \begin{bmatrix} L^I & \begin{bmatrix} L g_j(\mathbf{x}_i) \end{bmatrix}_{N_I \times M} \end{bmatrix},$$

$$\mathcal{A}_2 \equiv \begin{bmatrix} A^I & \begin{bmatrix} g_j(\mathbf{x}_i) \end{bmatrix}_{N_I \times M} \\ B & \begin{bmatrix} L_B g_j(\mathbf{x}_{N_I+i}) \end{bmatrix}_{N_B \times M} \\ \begin{bmatrix} g_i(\mathbf{x}_j) \end{bmatrix}_{M \times N} & 0_{M \times M} \end{bmatrix},$$

A few remarks should be made about the method:

- The matrix \mathcal{A} (or \mathcal{A}_2) usually becomes ill-conditioned as the number of nodes increases. This is a common problem when RBFs of global support are used [15].

- For the Dirichlet problem, the matrix \mathcal{A} has been proved to be invertible for most RBFs, and conditions that guarantee that \mathcal{A}_2 is nonsingular are known — see, e.g., [16, 17]. For $b \neq 0$ there is no proof that these matrices are invertible for any choice of nodes. We point out however, that for all numerical experiments we performed the matrices were nonsingular.
- The eigenvalue system is of size N_I , the number of interior nodes, although as an intermediate step one must invert a matrix of size N , the total number of nodes.
- One could rewrite the matrix eigenvalue system using the “inverse RBF operator”. In this case one would seek the eigenpairs $(\nu, \tilde{\mathbf{u}}^I)$ of the matrix H_ϕ ,

$$H_\phi \equiv A^I \begin{bmatrix} L^I \\ B \end{bmatrix}^{-1} \begin{bmatrix} I_{N_I \times N_I} \\ 0_{N_B \times N_I} \end{bmatrix}.$$

The approximate eigenvalues and eigenvectors of (1) would then be $1/\nu$ and $\tilde{\mathbf{u}}^I$, respectively.

Another approach is to write the finite-dimensional problem as a generalized eigenvalue problem. The idea is to substitute the RBF approximation (3) into the eigenvalue problem (1), leading to the following system:

$$\begin{bmatrix} L^I \\ B \end{bmatrix} \boldsymbol{\alpha} = \lambda \begin{bmatrix} A^I \\ 0_{N_B \times N} \end{bmatrix} \boldsymbol{\alpha}.$$

In this case, one would seek the generalized eigenvalues and eigenvectors of these matrices. This system is of size N , not N_I , but unlike L_ϕ , does not require a matrix inversion. Notice that in principle the accuracy of the approximation

does not depend on how the eigenpairs of the finite-dimensional problem are computed, but on the RBF and the set of nodes used. The generalized eigenvalue problem also suffers from ill-conditioning.

3.1 Numerical results

We tested the algorithm for the Laplacian operator. We computed the eigenmodes of a disk of radius π with Dirichlet and Neumann boundary conditions. We used multiquadric RBFs ($\phi(r) = \sqrt{c^2 + r^2}$) to generate the results and considered the expansion (7) with $M = 1$ and $g_1 = 1$.

Results are presented for the shape parameter $c = 3$. Increasing the value of c , in general, improves accuracy, but it worsens the matrix condition number. In [18], Cheng et al. establish by numerical experiments the error estimate $O(\vartheta\sqrt{c}/h)$, where $0 < \vartheta < 1$ and h is the mesh size, and that the matrix condition number is dependent on the parameter c/h . More information on selecting the parameter c can be found in [12, 19].

We count repeated eigenvalues and denote the exact j th eigenvalue by $\lambda^{(j)}$, $0 < \lambda^{(1)} \leq \lambda^{(2)} \leq \dots$. We exclude the zero eigenvalue of the Neumann problem, this eigenvalue has been computed to at least 11 accurate digits in our experiments. For an RBF-computed eigenvalue we write $\lambda_N^{(j)}$ and define the mesh size by

$$h \equiv \max_{i=1\dots N} \left\{ \min_{\substack{j=1\dots N \\ j \neq i}} \|x_i - x_j\|_2 \right\}.$$

Figure 2 shows the relative error, $|\lambda^{(j)} - \lambda_N^{(j)}|/\lambda^{(j)}$, in selected eigenvalues of the disk as function of $2\pi/h$. For the Dirichlet problem, the 3rd, 5th, 8th and 12th are repeated eigenvalues and the errors in these are not shown. Similarly,

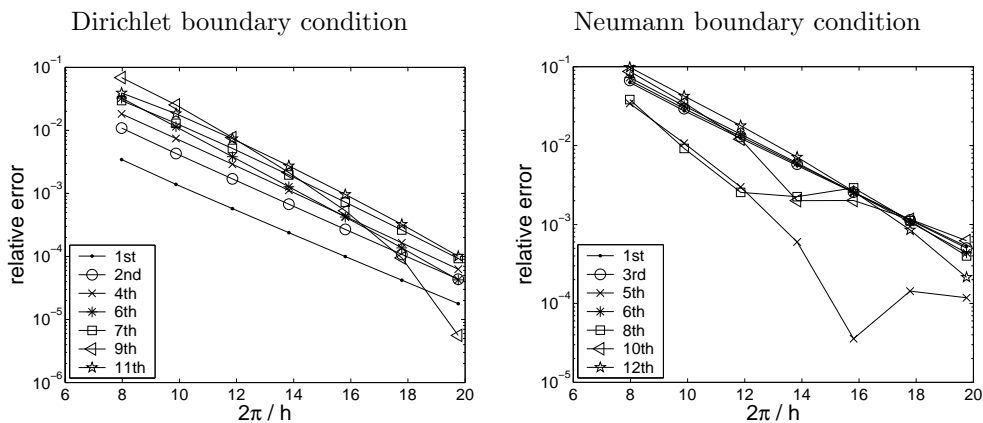


Figure 2: Relative error in selected eigenvalues of the disk.

for the Neumann problem we only show the error in distinct eigenvalues. We note that the lower eigenvalues are usually resolved more accurately than higher ones for the Dirichlet problem, but not for the Neumann problem where in most cases the 5th eigenvalue was most accurate among the first 12. As expected, the error presents exponential decay for the data used.

In order to obtain more accurate results, due to the constraint in the matrix condition number, one typically decreases the value of c and increases N . Since the work required to compute the solution is $O(N^3)$, this approach becomes computationally costly for large values of N .

4 Boundary treatment

RBF approximations are, in general, inaccurate near the boundary [2, 3, 7]. In this section we consider two techniques for improving accuracy near boundaries.

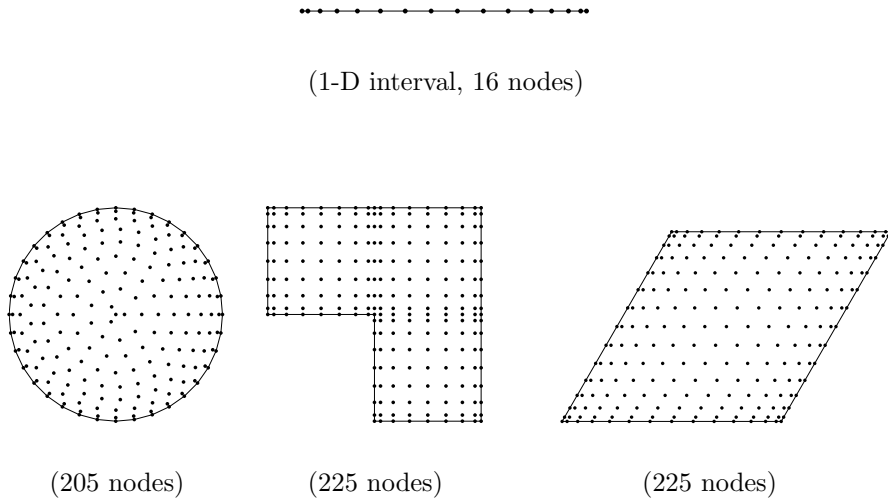


Figure 3: Boundary clustering.

4.1 Boundary clustering of nodes

Clustering of nodes near the boundary was found to be very successful in [7]. Clustering in a 1-D interval is essential for a high-degree polynomial interpolation to be successful. Chebyshev points, given by $\cos(j\pi/N)$, $j = 0, 1, \dots, N$ on $[-1,1]$, are commonly used to avoid large errors near the boundary for spectral methods based on polynomials. This motivates clustering the nodes more densely at boundaries for RBFs. In [7] numerical experiments were run based on nodes in $[-1,1]$ with density proportional to $(1-x^2)^{-\gamma}$. The case $\gamma = 0$ gives equispaced nodes, $\gamma > 0$ clusters nodes toward the endpoints, and $\gamma = 0.5$ gives the Chebyshev points; see [20] for more detail.

Figure 3 shows node distributions obtained with $\gamma = 0.4$. On top, the nodes on a 1-D interval are shown. Using these points, it is possible to generate nodes in 2-D regions as presented for the disk, triangle, and L-shaped region.

4.2 Collocation of the PDE on the boundary

The idea of adding equations obtained via collocation of the PDE on the boundary was introduced for boundary-value problems in [2]. We shall explore this approach in connection with the eigenvalue problem.

In order to add equations, an extra set of centers is needed. We add N_B centers outside the domain and adjacent to the boundary, so that $N = N_I + 2N_B$. In Figure 4, we show uniformly distributed nodes for the disk: the dots represent collocation nodes and the open circles represent centers.

The implementation of this scheme is straightforward. For $b \neq 0$ in (2), one just needs to consider the boundary collocation nodes as both boundary points and interior points (in the sense that both equations in (1) should be satisfied). The resulting L_ϕ matrix has the same structure presented previously.

For the Dirichlet boundary condition this simple procedure breaks down since $Lu = \lambda u$ implies that the matrix \mathcal{A} (or \mathcal{A}_2) would be singular. This difficulty can be avoided by rewriting the matrix

$$L_\phi \equiv L^I \mathcal{A}_3^{-1} \begin{bmatrix} I_{N_I \times N_I} \\ 0_{2N_B \times N_I} \end{bmatrix}, \quad \mathcal{A}_3 \equiv \begin{bmatrix} A^I \\ \left[L\phi(\|\mathbf{x}_{N_I+i} - \mathbf{y}_j\|_2) \right]_{N_B \times N} \\ B \end{bmatrix}.$$

4.3 Numerical results

We now compare the boundary treatment techniques for the test problem described in section 3.1. We adopted the following abbreviations: BC for boundary clustering of nodes and PDECB for collocation of the PDE on the boundary. Clustering of nodes was obtained using $\gamma = 0.4$.

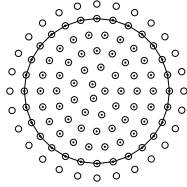


Figure 4: Example of distribution of centers (circles) and collocation nodes (dots) in a disk for collocation of the PDE on the boundary.

Figure 5 presents the maximum relative error over the 12 first eigenvalues, $\max_{1 \leq j \leq 12} |\lambda^{(j)} - \lambda_N^{(j)}| / \lambda^{(j)}$, for several values of N . The spectral convergence can be verified in the graphs of the error versus $2\pi/h$ (Fig. 5 left). We also plotted the error versus N (Fig. 5 right) since the work needed to compute the solution depends on N .

Both BC and PDECB improved the solution, BC giving the most accurate results of the two schemes. Combining the two techniques did not improve the solution over BC alone for the Dirichlet problem. For the Neumann problem, the combination resulted in better results. Comparing the results for the Dirichlet problem and for the Neumann problem we note that the results for the Dirichlet problem are, in most cases, more accurate than for the equivalent Neumann problem. We believe that the reason is that the resolution near the boundary plays a more important role for the Neumann problem since the derivatives of the expansions are needed at the boundary.

In Figure 6 we compare the performance of the RBF method to a spectral method and second-order finite elements. For the spectral scheme we used the algorithm described in [21], which uses Chebyshev-pseudospectral approxima-

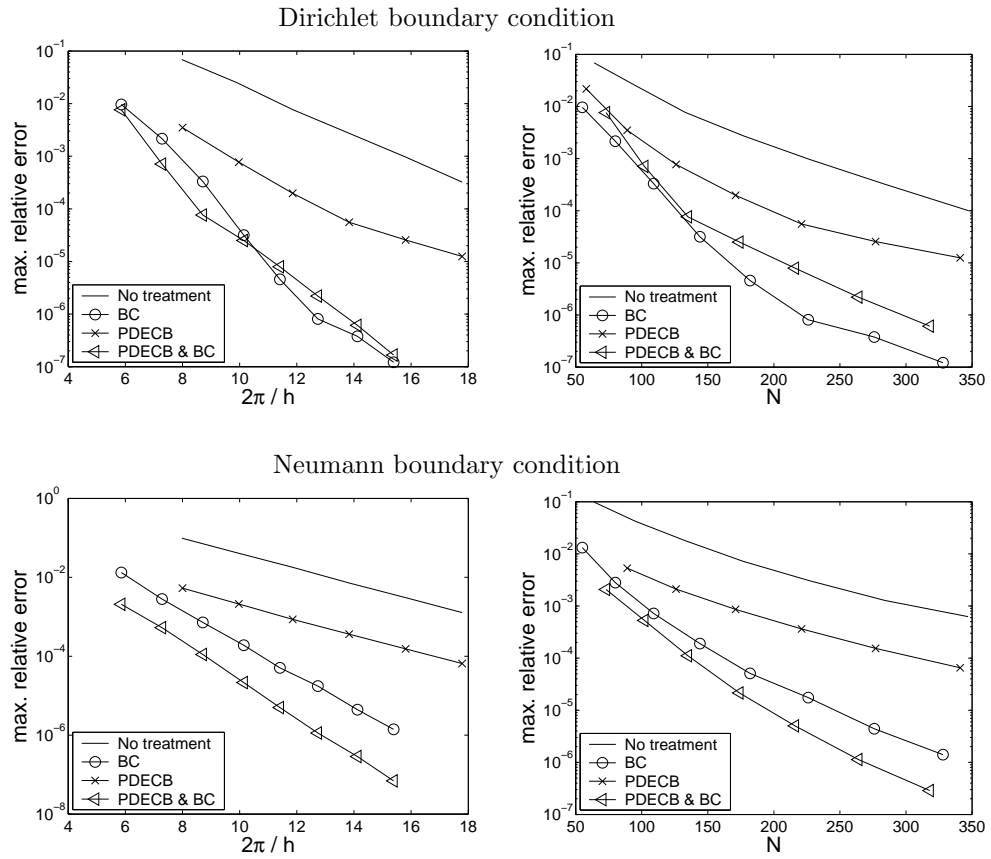


Figure 5: Maximum relative error over the first 12 eigenvalues of the disk.

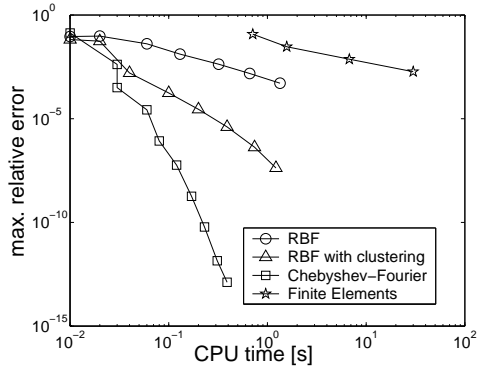


Figure 6: Maximum relative error over the first 12 eigenvalues versus CPU time for the disk with Dirichlet boundary condition.

tions in the radial direction and Fourier-pseudospectral approximations in the angular component. The finite element results were obtained with the PDE Toolbox for MATLAB. We used a 400MHz Linux PC to generate this data and all algorithms were implemented in MATLAB. Although the RBF method did not converge as fast as the spectral method (which is able to exploit the special structure of the disk), its performance was significantly better than the low-order finite element method.

5 Corner singularities

We now turn our attention to the eigenvalue problem in 2-D regions with corners and assume that L is the Laplacian operator. In a corner with interior angle π/φ an eigenfunction has a particular singular behavior if φ is not integer. For the L-shaped region, for instance, the singularity occurs at the reentrant corner. Generic numerical procedures are inefficient because of the loss of smoothness

at such corners. In particular, a typical RBF approximation gives a very poor approximation of an eigenfunction near a singularity. Clustering of points at the reentrant corner and collocation of the PDE on the boundary did not prevent poor convergence rates in our numerical experiments.

In order to improve our numerical scheme, we exploit the local behavior of the eigenfunction at a corner of the boundary. Let (r, θ) be polar coordinates originating from a corner. An eigenfunction u of (1) with Dirichlet boundary condition can be represented as

$$u(r, \theta) = \sum_{n=1}^{\infty} c_n J_{n\varphi}(\sqrt{\lambda}r) \sin(n\varphi\theta), \quad (8)$$

where J_ν is a Bessel function of first kind.

This information was used by Fox, Henrici, and Moler [8] to compute the eigenvalues of the L-shaped region by truncating (8) and requiring the trial solution to be zero at collocation points along the boundary. The method then consists in finding the zeros of the determinant of the resulting matrix which depends nonlinearly on λ . However, as pointed out in [10], as the number of terms in the truncated series is increased the matrix becomes nearly singular and obtaining the true eigenvalues becomes numerically impossible, although with special care this issue can be overcome [22]. The algorithm used by Driscoll in [10] uses domain decomposition and treats the corner expansion locally rather than globally, avoiding this difficulty but making the implementation more complex.

The modification in the RBF-method we propose here is easy to implement and yet avoids degradation of the solution at singular corners. We consider the

ascending series

$$J_\nu(z) = \left(\frac{1}{2}z\right)^\nu \sum_{k=0}^{\infty} \frac{\left(-\frac{1}{4}z^2\right)^k}{k!\Gamma(\nu+k+1)},$$

so we have that (8) becomes

$$u(r, \theta) = \sum_{n=1}^{\infty} \sum_{k=0}^{\infty} b_{nk} r^{n\varphi+2k} \sin(n\varphi\theta),$$

where the coefficients b_{nk} are independent of r and θ .

Motivated by the last expansion, we add terms of the form $r^{n\varphi+2k} \sin(n\varphi\theta)$ to the RBF approximation, i.e., in (7) we let $g_i = r^{n\varphi+2k} \sin(n\varphi\theta)$, where n and k are chosen appropriately so that the smallest powers of r are used. We believe that these extra terms help to capture the singular behavior of an eigenfunction at a corner. For the Neumann problem, we have that

$$u(r, \theta) = \sum_{n=0}^{\infty} \sum_{k=0}^{\infty} b_{nk} r^{n\varphi+2k} \cos(n\varphi\theta),$$

which suggests a similar modification.

We note that in our numerical experiments the matrix \mathcal{A}_2 obtained with the augmentation above was nonsingular and that ill-conditioned formulations may arise if the number of singular terms is large compared to the number of collocation nodes.

We believe that a similar singular term augmentation could be applied to RBF approximations of singular boundary value problems and problems in which the nature of the boundary condition changes abruptly, when the expansion of the singular part of the solution is known a priori [23].

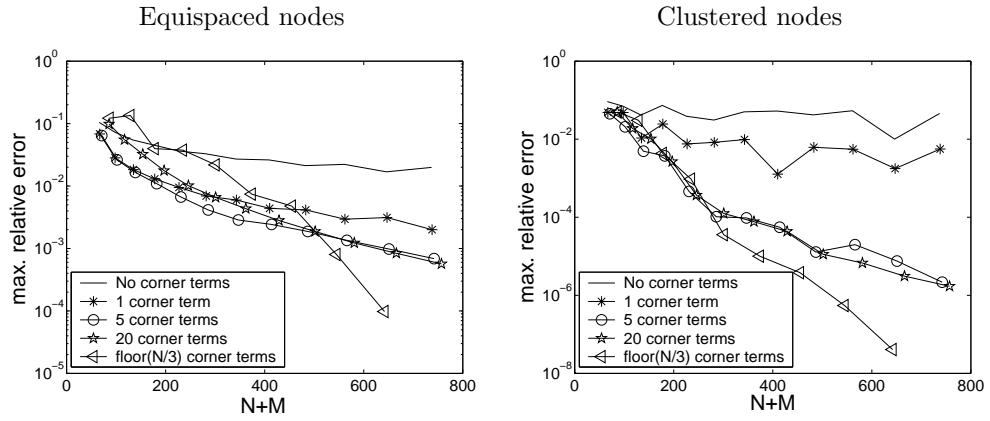
5.1 Numerical results

We considered two regions with corner singularities in our numerical experiments: the L-shaped region of vertices $(0, \pi/2)$, $(\pi/2, \pi/2)$, $(\pi/2, 0)$, $(\pi, 0)$, (π, π) and $(0, \pi)$, and the rhombus with supplementary angles 60° and 120° and sides of length π . We also used multiquadric RBFs to generate the results, with $c = 0.6$ for the L-shaped region and $c = 1.2$ for the rhombus.

The maximum relative error over the first 12 eigenvalues of the L-shaped region is presented in Figure 7 for several values of N and M . We note that the plain RBF expansion (3) does not converge and that clustering nodes near the singularity worsens the approximations for both Dirichlet and Neumann boundary conditions. Adding terms that exploit the reentrant corner information is essential for good approximations. In most cases, when only a few corner terms were used (1 to 20 terms) the rate of convergence appeared to be algebraic. Moreover, augmentation by only 1 corner term was not enough to avoid divergence when clustered nodes were used. The best results were obtained when the number of corner terms used was proportional to the number of nodes. In Fig. 7 we present results for $M \approx N/3$.

Figure 8 shows the contour plot of the 20th eigenfunction of the L-shaped region. The graph on the left presents the 20 contour lines obtained with the PDE Toolbox. The graph on the right is the RBF approximation generated with 279 clustered nodes and 103 corner terms. The finite element approximation was obtained with 4064 triangles. To compute the first 20 eigenmodes, the finite element scheme took approximately 11 seconds and the RBF method 3.8 seconds. The 20th eigenvalue was computed to 3 accurate digits with RBFs and

Dirichlet boundary condition



Neumann boundary condition

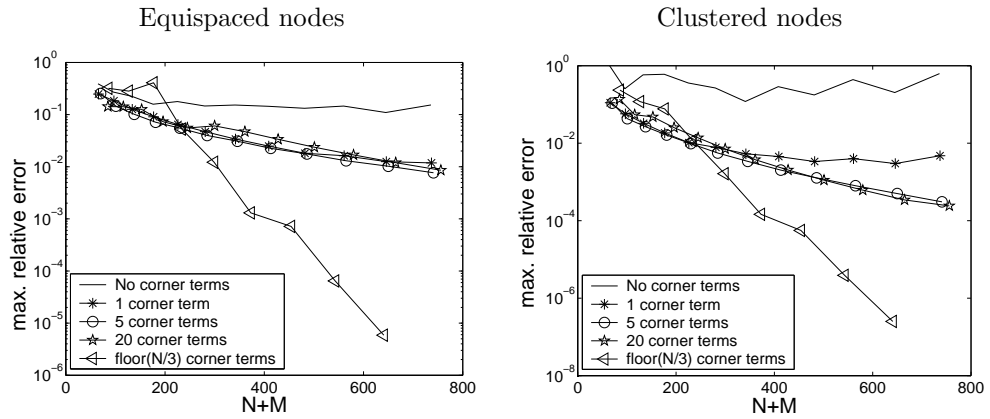


Figure 7: Maximum relative error over the first 12 eigenvalues of the L-shaped region with and without corner terms augmentation.

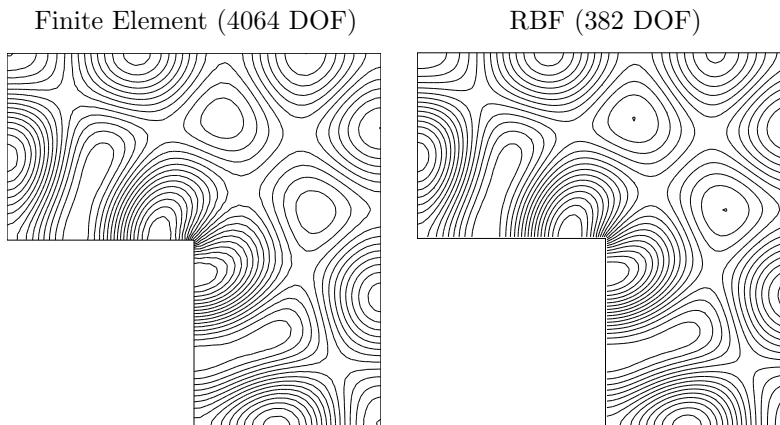


Figure 8: Contour plot of the 20th eigenfunction of the L-shaped region with Neumann boundary condition (20 contour lines).

to 2 accurate digits with the finite element method.

Our final test region is the rhombus. This region has two singular corners with angle $2\pi/3$. For the Dirichlet problem, the eigenfunctions that are anti-symmetric (about the shorter diagonal) are smooth since they be constructed using the modes of a equilateral triangle [24]. Other eigenfunctions present singular behavior, as it is the case of the first mode. Although this singularity is not as strong as it is in a reentrant corner, it still results in poor convergence rates for global methods that use smooth functions to approximate the solution. In fact, in [6] an algebraic convergence rate is predicted when RBFs are used to interpolate such modes. Our results show that this behavior can be avoided by singular corner augmentation.

Figure 9 shows the error in the first eigenfunction of the rhombus. The errors presented range from 0 (white) to the maximum absolute error (black) indicated

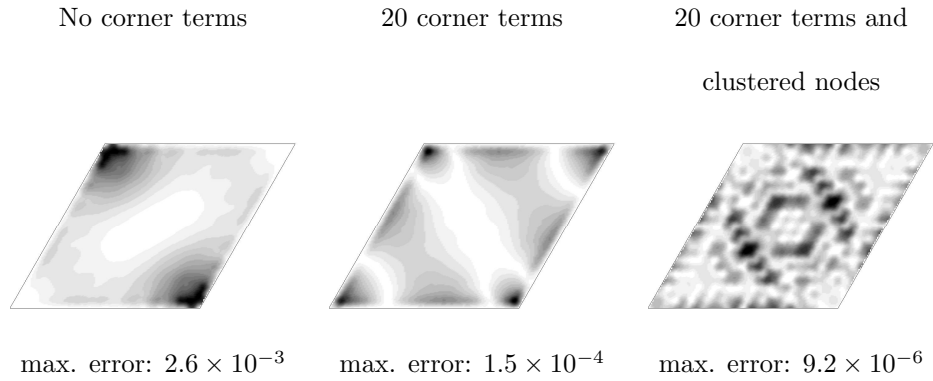


Figure 9: Error of the computed first eigenfunction of the rhombus with Dirichlet boundary condition, $N = 225$.

below each plot. One can see that the error is larger at the singular corners if the standard RBF expansion is used (left). When corner terms are added (center), the error decreases in magnitude and becomes more evenly distributed but it is still larger near the boundary. By using corner terms and clustering nodes more densely near the boundary (right) the error becomes evenly distributed in the entire domain.

Figure 10 presents the relative error of the first eigenvalue of the rhombus for several values of N and M . Although convergence can still be achieved without singular terms, the best results were obtained with corner-terms augmentation. We used terms from both corners evenly. In this case, adding few terms (2 to 20 terms) was enough to obtain good convergence rates.

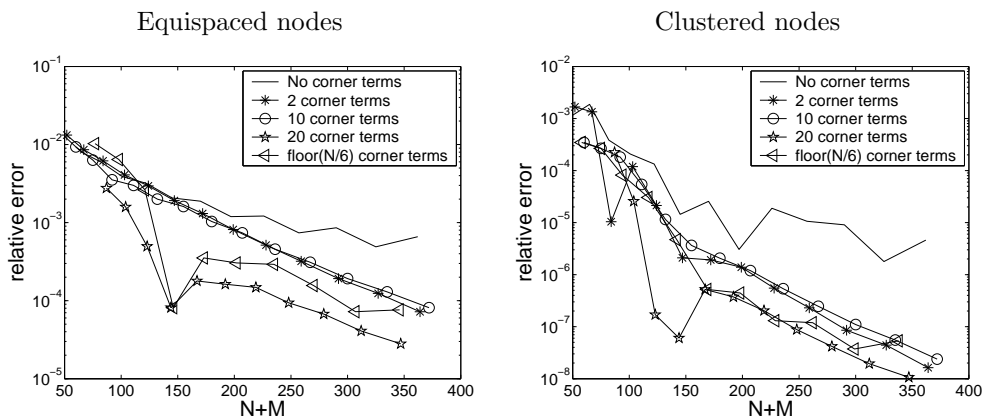


Figure 10: Relative error of the first eigenvalue of the rhombus with and without corner terms augmentation (Dirichlet boundary condition).

6 Conclusion

An RBF-based method has been presented for the eigenvalue problem for elliptic operators. The continuous problem is replaced with a finite-dimensional eigenvalue problem. Special attention is given for the approximation near the boundaries in order to improve the accuracy of the method. For 2-D regions with corner singularities, terms were added to the RBF approximation. These terms are obtained from the general expansion of eigenfunctions at a corner.

Our numerical experiments show that the RBF method can be used effectively for solving eigenvalue problems. The results computed with the boundary treatment techniques showed considerable improvement in accuracy. In most cases, boundary clustering of nodes gave better results than the collocation of the PDE on the boundary. We note, however, that the latter is easier to implement in irregular domains. For the L-shaped region and the rhombus, the

inclusion of singular terms was found to be essential for good convergence rates.

We believe that the techniques presented here can still be improved. For instance, some numerical experiments suggest that adding more centers outside the domain (as suggested in [7]) would improve accuracy and the conditioning of the problem. Another open question is how to cluster nodes near boundaries for general irregular domains and what is the “optimal” clustering of nodes.

References

- [1] E.J. Kansa, Multiquadrics - A scattered data approximation scheme with applications to computational fluid dynamics - II. Solutions to hyperbolic, parabolic, and elliptic partial differential equations. *Computers Math. Applic.* 19 (8-9) 147-161 (1990).
- [2] A.I. Fedoseyev, M. J. Friedman, and E. J. Kansa, Improved multiquadric method for elliptic differential equations via PDE collocation on the boundary. *Computers Math. Applic.* 43 (3-5) 439-455 (2002).
- [3] E. Larsson and B. Fornberg, A numerical study of some radial basis function based solution methods for elliptic PDEs. *Computers Math. Applic.*, to appear.
- [4] M. Sharan, E. J. Kansa, and S. Gupta, Application of the multiquadric method for numerical solution of elliptic partial differential equations. *Appl. Math. Comput.* 84 (2-3) 275-302 (1997).

- [5] W.R. Madych and S. A. Nelson, Multivariate interpolation and conditionally positive definite functions. II. *Math. Comp.* 54 (189) 211-230 (1990).
- [6] J. Yoon, Spectral approximation orders of radial basis function interpolation on the Sobolev space. *SIAM J. Math. Anal.* 33 (4) 946-958 (2001).
- [7] B. Fornberg, T. A. Driscoll, G. Wright, and R. Charles, Observations on the behavior of radial basis function approximations near boundaries. *Computers Math. Applic.* 43 (3-5) 473-490 (2002).
- [8] L. Fox, P. Henrici, and C. Moler, Approximations and bounds for eigenvalues of elliptic operators. *SIAM J. Numer. Anal.*, 4 (1) 89-102 (1967).
- [9] J. Descloux, M. Tolley, An accurate algorithm for computing the eigenvalues of a polygonal membrane. *Comput. Methods Appl. Mech. Engrg.* 39 (1) 37-53 (1983)
- [10] T.A. Driscoll, Eigenmodes of isospectral drums. *SIAM Rev.* 39 (1) 1-17 (1997).
- [11] M.D. Buhmann, Radial basis functions. *Acta Numerica* 9, 1-38 (2000).
- [12] T.A. Driscoll and B. Fornberg, Interpolation in the limit of increasingly flat radial basis functions. *Computers Math. Applic.* 43 (3-5) 413-422 (2002).
- [13] H. Wendland, Piecewise polynomial, positive definite and compactly supported radial functions of minimal degree. *Adv. in Comput. Math.* 4 (4) 389-396 (1995).
- [14] R.L. Hardy, Multiquadric equations of topography and other irregular surfaces. *J. Geophys. Res.* 76 (8) 1905-1915 (1971).

- [15] E.J. Kansa and Y. C. Hon, Circumventing the ill-conditioning problem with multiquadric radial basis functions: Applications to elliptic partial differential equations. *Computers Math. Applic.* 39 (7-8) 123-137 (2000).
- [16] C.A. Micchelli, Interpolation of scattered data: distance matrices and conditionally positive definite functions. *Constr. Approx.* 2 (1) 11-22 (1986).
- [17] M.J.D. Powell, The theory of radial basis function approximation in 1990. In *Numerical Methods of Approximation Theory* (W.A. Light, ed.), Oxford University Press, Oxford, 105-210 (1992).
- [18] A.H.-D Cheng, M.A. Golberg, E.J. Kansa, and G. Zammito, Exponential convergence and H-c multiquadric collocation method for partial differential equations. *Numer. Methods Partial Equations* 19 (5) 571-594 (2003).
- [19] S. Rippa, An algorithm for selecting a good value for the parameter c in radial basis function interpolation. *Adv. Comp. Math.* 11 (2-3) 193-210 (1999).
- [20] B. Fornberg, *A Practical Guide to Pseudospectral Methods*. Cambridge University Press, (1996).
- [21] L.N. Trefethen, *Spectral Methods in MATLAB*. SIAM, Philadelphia (2000).
- [22] T. Betcke and L.N. Trefethen, Private communications (2003).
- [23] Z. Yosibash, Numerical analysis on singular solutions of the Poisson equation in two-dimensions. *Comput. Mech.*, 20 (4) 320-330.
- [24] B.J. McCartin, Eigenstructure of the equilateral triangle, part I: the Dirichlet problem. *SIAM Rev.*, 45 (2) 267-287 (2003).